Predictability of the quasi-biennial oscillation and its northern winter teleconnection on seasonal to decadal timescales

Adam A. Scaife[1], Maria Athanassiadou[1], Martin Andrews[1], Alberto Arribas[1], Mark Baldwin[2], Nick Dunstone[1], Jeff Knight[1], Craig MacLachlan[1], Elisa Manzini[3], Wolfgang A. Müller[3], Holger Pohlmann[3], Doug Smith[1], Tim Stockdale[4], and Andrew Williams[1]

[1]Met Office Hadley Centre, Exeter, UK, [2]Department of Mathematics and Computer Science, University of Exeter, Exeter, UK, [3]Max Planck Institute for Meteorology, Hamburg, Germany, [4]European Centre for Medium-Range Weather Forecasts, Reading, UK

Abstract The predictability of the quasi-biennial oscillation (QBO) is examined in initialized climate forecasts extending out to lead times of years. We use initialized retrospective predictions made with coupled ocean-atmosphere climate models that have an internally generated QBO. We demonstrate predictability of the QBO extending more than 3 years into the future, well beyond timescales normally associated with internal atmospheric processes. Correlation scores with observational analyses exceed 0.7 at a lead time of 12 months. We also examine the variation of predictability with season and QBO phase and find that skill is lowest in winter. An assessment of perfect predictability suggests that higher skill may be achievable through improved initialization and climate modeling of the QBO, although this may depend on the realism of gravity wave source parameterizations in the models. Finally, we show that skilful prediction of the QBO itself does not guarantee predictability of the extratropical winter teleconnection that is important for surface winter climate prediction.

1. Introduction

The inherent timescale of atmospheric processes is generally considered to be too short to aid climate prediction on seasonal to decadal timescales [e.g., *Smith et al.*, 2012]. However, the tropical stratosphere represents a clear exception to this general rule. Theoretically, the tropical stratosphere has interannual memory [*Scott and Haynes*, 1998], and zonal wind anomalies can persist for many months. The very large and quasi-regular interannual fluctuations from the quasi-biennial oscillation (QBO) [*Veryard and Ebdon*, 1961; *Reed et al.*, 1961] could therefore provide one of the few purely atmospheric sources of climate predictability on seasonal to decadal timescales.

This study makes use of ensembles of seasonal to decadal forecasts to quantify prediction skill of the QBO. The large number of simulated years in these retrospective forecasts poses restrictions in the resolution of the climate model used due to limitations in computing resources. Such forecasts are generally made at climate model resolution of around 1° in the atmosphere. At this resolution, much of the gravity wave spectrum that drives the QBO remains unresolved [*Geller et al.*, 2013]. However, a few climate models, including the models used here, now successfully simulate the QBO through the combined forcing from resolved waves and the parameterization of nonorographic gravity wave momentum fluxes [*Scaife et al.*, 2000; *Giorgetta et al.*, 2002; *Scinocca et al.*, 2008].

Seasonal hindcasts for this study are provided by two systems. We first use output from the UK Met Office (UKMO) Global Seasonal forecast system [*Arribas et al.*, 2011]. We use the fifth generation of this system, GloSea5, which is currently used for operational long-range forecasting. The climate model at the core of the forecast system is the third Hadley Centre Global Environmental Model version 3 (HadGEM3) with atmospheric resolution of 0.83° longitude by 0.55° latitude, 85 quasi-horizontal atmospheric levels, and an upper boundary at 85 km near the mesopause [*Walters et al.*, 2011]. The ocean resolution is 0.25° globally in both latitude and longitude with 75 quasi-horizontal levels [*Scaife et al.*, 2011]. Hindcasts are used for the period 1996 to 2009 with nine members per start date. Members from the same start date differ only by stochastic physics. Initial atmospheric and land surface data are taken from ERA-Interim observational reanalyses, and initial conditions for the global ocean and sea ice concentration are from the Forecasting Ocean Assimilation Model data
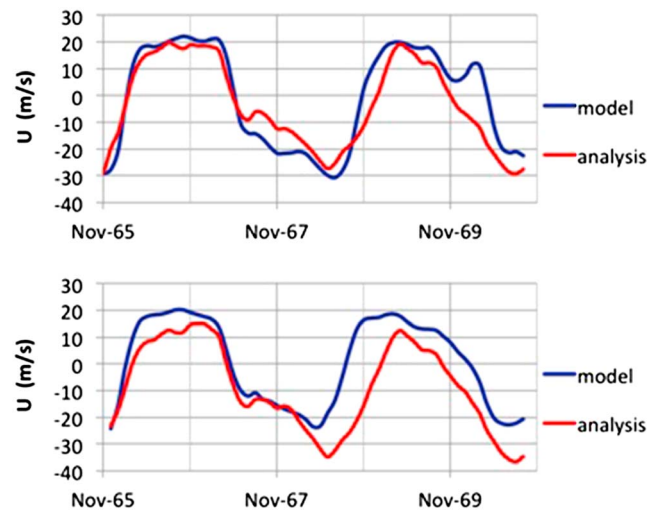
Figure 1. Example of observational analysis and multiannual forecasts of the `30 hPa monthly mean zonal wind (ms^{-1}) near the equator for the (top) UKMO DePreSysv2 and (bottom) MiKlip models. Example forecasts starting in 1965 are shown against the respective observational analysis.

assimilation system. We also use output from the ECMWF System 4 seasonal forecasting system [*Molteni et al.*, 2011]. This uses a T255 resolution spectral model, with a corresponding grid spacing of about 80 km, and 91 levels in the vertical with an upper boundary at 0.01 hPa. Ocean resolution is 1° with meridional refinement to 0.3° near the equator. Initial conditions are taken from ERA-Interim or, for the ocean, from Ocean Reanalysis System (ORAS4) [*Balmaseda et al.*, 2012]. Hindcasts are available from 1981 to 2010, with a 51-member ensemble per start date.

Decadal hindcasts for this study are provided by two systems. The first set is from the UKMO decadal prediction system [*Smith et al.*, 2007, 2010]. We use output from the second generation of this system, DePreSysv2, which also uses the HadGEM3 climate model. The decadal predictions extend out to several years ahead but are run at lower resolution with latitude-longitude spacing of 1.25° latitude by 1.875° longitude and the same 85 model levels extending to 0.01 hPa. The ocean resolution is 1°. The DePreSysv2 hindcasts consist of four-member ensembles starting from 1 November every year from 1960 to 2006. The second set is from the Mittelfristige Klimaprognosen (MiKlip) decadal climate prediction system [*Pohlmann et al.*, 2013]. This is based on the Max-Planck-Institut-Earth System Model (MPI-ESM) coupled climate model [*Giorgetta et al.*, 2013; *Stevens et al.*, 2013; *Jungclaus et al.*, 2013]. The mixed resolution version MPI-ESM-mixed resolution (atmosphere: T63L95, ocean: 0.4degL40) is used here, with five-member ensembles initialized on 1 January every year between 1961 and 2012. The representation of the QBO in this model is discussed in *Krismer et al.* [2013]. Decadal hindcasts are started from a combined atmospheric and oceanic initialization. The atmospheric fields (surface pressure and spectral temperature, vorticity, and divergence) are taken from the reanalyses ERA-40 [*Uppala et al.*, 2005] for the period 1960–1989 and ERA-Interim [*Dee et al.*, 2011] for the period 1990–2012, respectively. The oceanic component is initialized with temperature and salinity anomalies from the oceanic reanalysis ORAS4 [*Balmaseda et al.*, 2012].

In addition to assessing prediction skill of the QBO on seasonal to decadal timescales, we also look at the predicted impact on surface winter climate. Numerous studies have identified an apparent extratropical response to the QBO in winter [*Ebdon*, 1975; *Holton and Tan*, 1980], and some analyses suggest that the QBO could be a useful important additional source of skill for surface climate predictions [*Thompson et al.*, 2002; *Boer and Hamilton*, 2008; *Folland et al.*, 2011; *Smith et al.*, 2012]. We therefore also assess whether the influence of the QBO on extratropical surface winter climate is reproduced in initialized seasonal to decadal predictions.
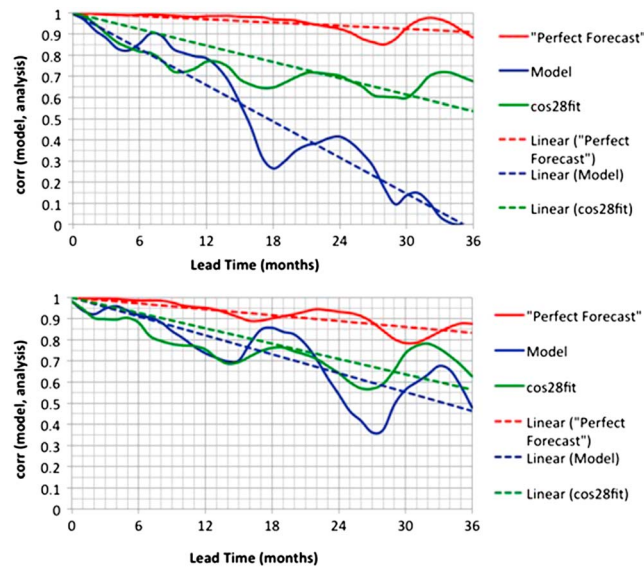
2. Predictability of the Quasi-Biennial Oscillation

We use the 30 hPa monthly mean zonal wind near the equator as a standard diagnostic of the state of the QBO. Example forecasts of the QBO are shown in Figure 1 for the UKMO DePreSysv2 and MiKlip systems. These example forecasts were initialized in late 1965 and were free running thereafter. Both the amplitude and the period are reasonably represented in these forecasts, and the asymmetry between a strong easterly phase ($\sim-30\,ms^{-1}$) and a weaker westerly phase ($\sim20\,ms^{-1}$) is represented, at least in the UKMO DePreSysv2 decadal forecasts.

We now assess predictability of the QBO using retrospective forecasts initialized in the period 1960–2006. The blue lines in Figure 2 show correlation scores for ensemble mean forecasts measured against observational analyses for the UKMO DePreSysv2 and MiKlip decadal forecast systems. The skill of these QBO

Figure 2. Predictability of the QBO in (top) UKMO and (bottom) MiKlip using decadal forecasts over 1960–2006. Correlation scores are plotted as a function of lead time for monthly and zonally averaged values of equatorial wind at 30 hPa verified against observational analyses (blue). Perfect predictability scores calculated by replacing the observational analysis with single ensemble members (red) and simple forecasts based on a 28 month sinusoid (green) starting from the observed phase. UKMO forecasts were initialized in November while MiKlip forecasts were initialized in January. Dashed lines show linear least squares fits.

predictions remains high at very long lead times and is higher than other highly predictable modes of climate variability such as El Niño–Southern Oscillation [*Fedorov et al.*, 2003; *Barnston et al.*, 2012]. Correlation scores exceed 0.8 at prediction times up to 6 months. At 12 months lead time the correlations are still above 0.7, and positive correlations are maintained out to years ahead in both forecast systems (Figure 2), remaining significant out to 4 years ahead in the MiKlip forecasts [c.f. *Pohlmann et al.*, 2013].

A complementary view to these deterministic correlation scores is a probabilistic assessment, for example, of the success and failure rates for predicting the phase of the QBO. Table 1 shows the probability of correct prediction of the sign of the QBO in the first three winters, from the UKMO DePreSysv2, for forecasts started in early November. High scores are shown for the first three winters, with decaying but above climatological probability of correctly predicting the sign of the QBO even in the third winter.

Verification against observational analysis is an important guide to the level of forecast skill that might be achievable with current systems, but what potential is there for higher skill? To answer this question we first use a very simple statistical model of the QBO. Assuming that the QBO is a regular 28 month sinusoidal oscillation, we calculate correlation scores given the initial phase of the oscillation. The initial phase is calculated as $2\pi n/28$ where n is the number of months since the last QBO maximum phase (either E or W). The green lines in Figure 2 demonstrate the high predictability of the QBO based on the above model. This simple method yields skill at least as high as that found in dynamical prediction systems, especially for timescales beyond 1 year, and demonstrates that the QBO is regular enough to have a high degree of inherent predictability.

Observational analyses used to initialize the forecasts inevitably contain errors due to imperfect observations, and the models themselves may contain errors, for example, in the average period of the

Table 1. Probability of Correct Prediction of the Sign of the Winter QBO From UKMO Decadal Forecasts[a]

Forecast QBO Phase	Winter 1	Winter 2	Winter 3
Easterly	91%	79%	61%
Westerly	80%	84%	58%

[a]Given an ensemble mean forecast for QBO easterly or westerly phase in the coming three winters, the probability of this phase occurring in the respective winters is tabulated. Climatological forecasts would give 50% for each phase.
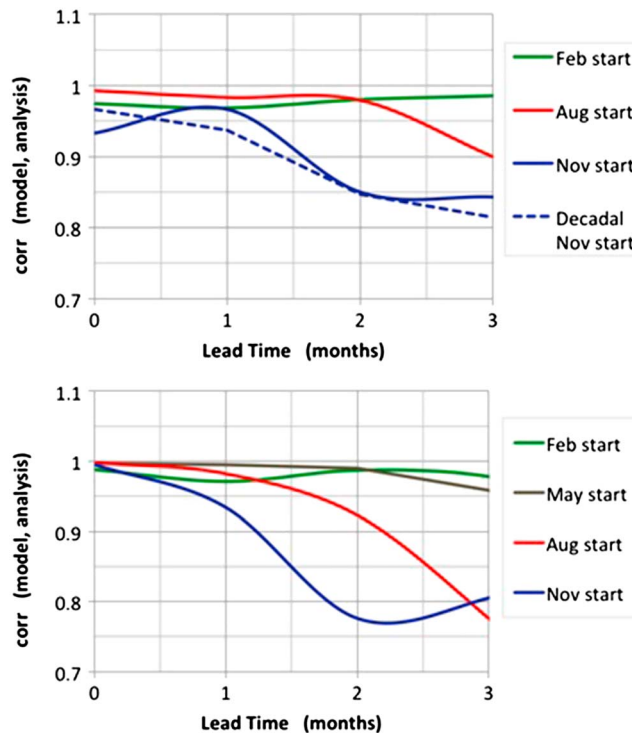
Figure 3. Predictability of the QBO in different seasons in independent sets of seasonal forecasts for the years 1996–2009. Correlation scores between forecasts and observational analyses of QBO winds at 30 hPa are plotted for forecasts beginning at the start of February (green), the start of May (brown), the start of August (red), and the start of November (blue). The dashed blue line shows the first few months of UKMO decadal forecasts which also began in November. (top) UKMO forecasts and (bottom) ECMWF forecasts.

QBO. We therefore estimate the theoretical maximum level of predictability in each forecast system by replacing the observations with each of the forecast ensemble members and repeating the skill calculation using the ensemble mean of remaining members. The result is shown by the red lines in Figure 2, which indicate that even higher levels of perfect predictability are present for the QBO in these forecast systems, with correlations exceeding 0.8 even 3 years ahead. We can therefore surmise that if initial condition errors and model errors in representing the QBO are reduced, then much higher levels of forecast skill may be achievable. Note, however, that perfect predictability estimates like this only have a bearing on actual forecasts to the extent that models are realistic. The QBO in these climate models is partly driven by a *constant source* of parameterized gravity waves from the lower atmosphere. The *filtering* of upward propagating waves by winds as they pass through the troposphere and lower stratosphere introduces significant variability in the wave fluxes of momentum arriving at the QBO in both models and observations [*Warner et al.*, 2005; *Ern and Preusse*, 2009]. *Unpredictable variations* in the *sources* of gravity waves from the troposphere, not currently represented in the forecast systems used here, may reduce the predictability of the QBO in practice. It could therefore be that perfect predictability scores here overestimate the scope for improvement.

3. Sensitivity to the Seasonal Cycle and QBO Phase

The forecasts examined so far included all years, with the QBO phase during initialization ranging from strong easterly to strong westerly. However, the QBO exhibits asymmetries between the easterly and westerly phases. In particular, the westerly phase is weaker in amplitude but propagates more rapidly down through the atmosphere than the easterly phase [*Dunkerton*, 1991] and these features can be reproduced in climate model simulations of the QBO [*Scaife et al.*, 2002; *Giorgetta et al.*, 2006]. How do these asymmetries affect the predictability of the QBO? To answer this question we split the forecasts used in Figure 2 into an east and a west category, depending on the phase of the QBO at the start of the forecast. Given the approximate reversal of QBO phase 1 year later, this means that westerly phases at the start of the forecasts are indicative of easterly QBO in the coming year, and vice versa. Both MiKlip and UKMO forecasts showed a hint of differences in skill over the following years depending on this initial phase (not shown), but while impending easterly phases showed slightly lower skill, differences were small and were not examined further.

The QBO forecasts examined so far covered the winter period and were from November or January initializations. Given the enhanced stalling, especially in winter during the easterly phase of the QBO, there may also be a seasonal dependence of QBO forecast skill. To test this we use seasonal forecasts initialized at different times of year. Correlation scores for QBO winds for forecasts that started in each season are
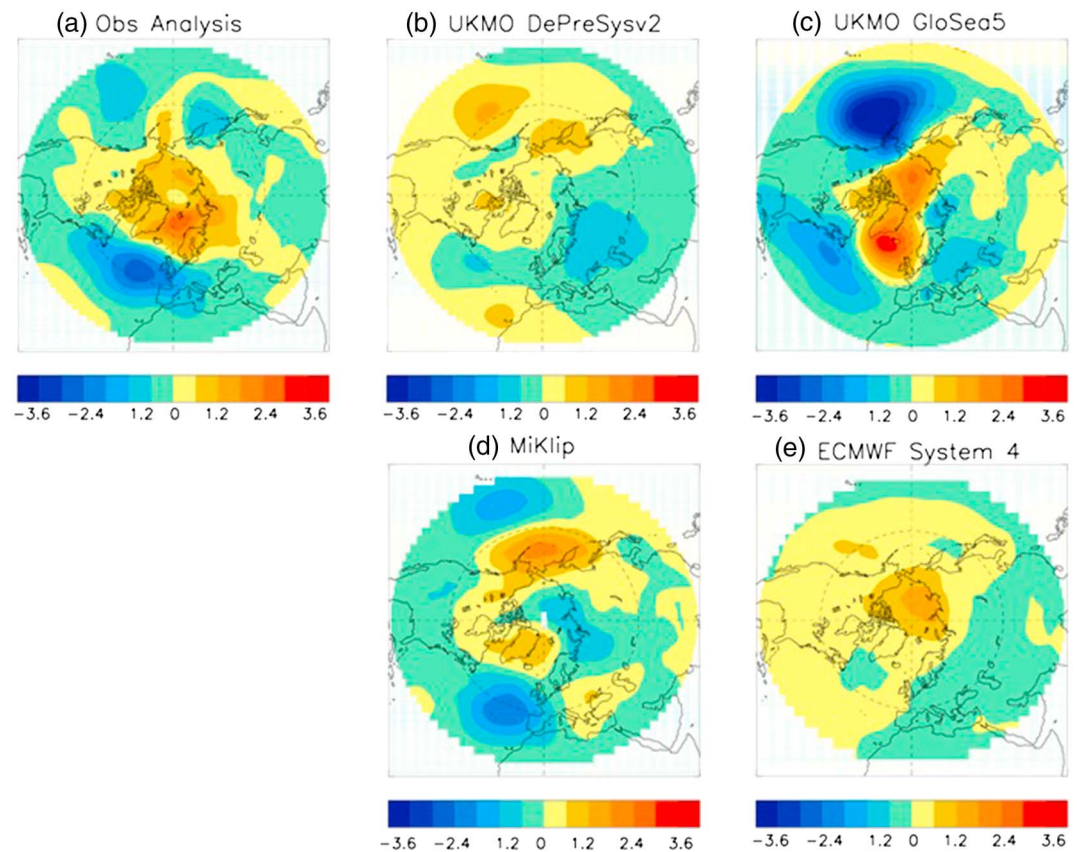
Figure 4. Winter teleconnections to the QBO. Sea level pressure signals (hPa) are shown as mean differences between easterly and westerly phases of the QBO in (a) UKMO observational analyses, (b) UKMO decadal hindcasts, (c) UKMO seasonal hindcasts, (d) MiKlip decadal hindcasts, and (e) ECMWF seasonal hindcasts. All panels are for the winter season from December to February inclusive. Units are hPa.

shown in Figure 3 using all phases of the QBO. It is apparent that forecasts for the winter season in both forecast systems are less skilful than those for spring or autumn. Similar to the dependence of skill on QBO phase, this seasonal cycle in forecast skill is consistent with irregular downward propagation of the QBO, limiting predictability in this season. This effect can also be seen by the rapidly declining skill of forecasts that started in November and August as they approach winter. This seasonal dependence also has consequences when comparing the skill in different forecast systems. Comparison of QBO skill in different systems need to be done from the same start date as in Figure 3 rather than from different start dates (e.g., MiKlip and UKMO in Figure 2).

4. Teleconnections to Boreal Winter Surface Climate

Evidence of possible impacts of the QBO at the surface is long known [e.g., *Ebdon*, 1975]. Moreover, despite the large amount of interannual variability in surface winter climate, recent estimates of QBO teleconnections appear to remain significant [*Boer and Hamilton*, 2008]. Enhanced sea level pressure gradients and stronger, northward shifted tropospheric jets occur under westerly QBO compared to easterly QBO conditions. While there has been some success in reproducing this surface teleconnection to the QBO in climate models [*Hamilton*, 1998; *Pascoe et al.*, 2005; *Yamashita et al.*, 2011], this is not generally the case and it is therefore important to continue to test climate prediction systems for their ability to reproduce the QBO signal in surface winter climate.

The surface winter signal from the QBO in observational analyses is shown in Figure 4a as the mean difference in winter sea level pressure between easterly and westerly cases (E-W). Higher than normal pressure over the Arctic and lower than normal pressure over the midlatitudes, particularly in the

Atlantic storm track region, indicate a more negative North Atlantic Oscillation/Arctic Oscillation in the easterly than the westerly QBO phase. The amplitude of this effect is several hPa, a sizeable fraction of the year-to-year variability itself (not shown). The QBO therefore appears to shift the sea level pressure by a significant proportion of the interannual standard deviation and could contribute to winter seasonal forecast skill [e.g., *Boer and Hamilton*, 2008; *Marshall and Scaife*, 2009; *Fereday et al.*, 2012].

The performance of the decadal and seasonal forecasts described above in reproducing the observed QBO surface teleconnection is shown in Figure 4. The UKMO decadal hindcasts cover the same period as the observed analysis but show only small and statistically insignificant differences in surface climate between the E and W phases of the QBO. MIKLIP decadal and ECMWF seasonal forecasts show some signature of the teleconnection, but it is very weak. UKMO seasonal forecasts show high pressure at high latitudes and low pressure at midlatitudes in the easterly minus westerly QBO composite. The sign and basic pattern of the teleconnection appears to be reproduced in these forecasts, with high pressure over the Arctic and lower pressure at midlatitudes, albeit with weaker than observed amplitude.

5. Conclusion

We have quantified levels of predictability of the QBO in initialized climate predictions on seasonal to decadal timescales. High levels of predictability were found in retrospective forecasts with correlations exceeding 0.7 at a lead time of 1 year. This basic result is insensitive to the details of the prediction system. We also find some sensitivity of the forecast skill to both the season and phase of the QBO at the start of the forecast. Forecasts leading into winter and starting in the westerly phase show the lowest subsequent skill. It would be interesting to extend this analysis to forecasts beginning in other calendar months to fully characterize the seasonal dependence of QBO prediction skill. There are also hints at potentially significant improvement from idealized estimates of predictability. However, these "perfect predictability" estimates may be different in models with a QBO that does not rely on parameterized gravity waves [e.g., *Kawatani et al.*, 2010] and it is not yet known whether including variability in gravity wave sources would make predictions less skilful by adding unpredictable variability or more skilful, for example, by improving the seasonal cycle in gravity waves [e.g., *Krebsbach and Preusse*, 2013]. Finally, despite success in predicting the QBO itself, only certain aspects of the QBO teleconnections to the surface climate are represented in many model forecasts as weak North Atlantic Oscillation/Arctic Oscillation-like pressure patterns. Further work is needed to robustly reproduce what appear to be sizeable QBO effects on surface winter climate in seasonal to decadal climate predictions.

References

Arribas, A., et al. (2011), The GloSea4 ensemble prediction system for seasonal forecasting, *Mon. Weather Rev.*, *139*, 1891–1910.
Balmaseda, M. A., K. Mogensen, and A. T. Weaver (2012), Evaluation of the ECMWF ocean reanalysis system ORAS4, *Q. J. R. Meteorol. Soc.*, *139*, 1132–1161, doi:10.1002/qj.2063.
Barnston, A. G., M. K. Tippett, M. L. L'Heureux, S. Li, and D. G. DeWitt (2012), Skill of real time seasonal ENSO model predictions during 2002-2011. Is Our Capability Increasing?, *Bull. Am. Meteorol. Soc.*, *93*, 631–651.
Boer, G., and K. Hamilton (2008), QBO influence on extratropical predictive skill, *Clim. Dyn.*, *31*, 987–1000.
Dee, D. P., et al. (2011), The ERA-Interim reanalysis: Configuration and performance of the data assimilation system, *Q. J. R. Meteorol. Soc.*, *137*, 553–597, doi:10.1002/qj.828.
Dunkerton, T. (1991), Non-linear propagation of zonal winds in an atmosphere with Newtonian cooling and equatorial wave driving, *J. Atmos. Sci.*, *48*, 236–263.
Ebdon, R. A. (1975), The quasi-biennial oscillation and its association with tropospheric circulation patterns, *Meteorol. Mag.*, *104*, 282–297.
Ern, M., and P. Preusse (2009), Wave fluxes of equatorial Kelvin waves and QBO zonal wind forcing derived from SABER and ECMWF temperature space-time spectra, *Atmos. Chem. Phys.*, *9*, 3957–3986.
Fedorov, A. V., S. L. Harper, S. G. Philander, B. Winter, and A. Wittenberg (2003), How predictable is El Niño?, *Bull. Am. Meteorol. Soc.*, *84*, 911–919, doi:10.1175/BAMS-84-7-911.
Fereday, D., A. Maidens, A. Arribas, A. Scaife, and J. R. Knight (2012), Seasonal forecasts of northern hemisphere winter 2009/10, *Env. Res. Lett.*, *7*, doi:10.1088/1748-9326/7/3/034031.
Folland, C. K., A. A. Scaife, J. Lindesay, and D. Stephenson (2011), How predictable is European winter climate a season ahead?, *Int. J. Climatol.*, doi:10.1002/joc.2314.
Geller, M., et al. (2013), A comparison between gravity wave momentum fluxes in observations and climate models, *J. Clim.*, doi:10.1175/JCLI-D-12-00545.1.
Giorgetta, M. A., E. Manzini, and E. Roeckner (2002), Forcing of the quasi-biennial oscillation from a broad spectrum of atmospheric waves, *Geophys. Res. Lett.*, *29*(8), 1245, doi:10.1029/2002GL014756.
Giorgetta, M. A., E. Manzini, E. Roeckner, M. Esch, and L. Bengtsson (2006), Climatology and forcing of the quasi-biennial oscillation in the MAECHAM5 model, *J. Clim.*, *19*, 3882–3901, doi:10.1175/JCLI3830.1.

Giorgetta, M. A., et al. (2013), Climate and carbon cycle changes from 1850 to 2100 in MPI-ESM simulations for the Coupled Model Intercomparison Project phase 5, *J. Adv. Model. Earth Syst.*, *5*, 572–597, doi:10.1002/jame.20038.

Hamilton, K. (1998), Effects of an imposed quasi-biennial oscillation in a comprehensive troposphere-stratosphere-mesosphere general circulation model, *J. Atmos. Sci.*, *55*, 2393–2418.

Holton, J. R., and H.-C. Tan (1980), The influence of the equatorial quasi-biennial oscillation on the global circulation at 50 mb, *J. Atmos. Sci.*, *37*, 2200–2208.

Jungclaus, J. H., N. Fischer, H. Haak, K. Lohmann, J. Marotzke, D. Matei, U. Mikolajewicz, D. Notz, and J. S. von Storch (2013), Characteristics of the ocean simulations in MPIOM, the ocean component of the MPI-Earth system model, *J. Adv. Model. Earth Syst.*, *5*, 422–446, doi:10.1002/jame.20023.

Kawatani, Y., S. Watanabe, K. Sato, T. J. Dunkerton, S. Miyahara, and M. Takahashi (2010), The roles of equatorial trapped waves and internal inertia–gravity waves in driving the quasi-biennial oscillation. Part I: Zonal mean wave forcing, *J. Atmos. Sci.*, *67*, 963–980.

Krebsbach, M., and P. Preusse (2013), Spectral analysis of gravity wave activity in SABER temperature data, *Geophys. Res. Lett.*, *34*, L03814, doi:10.1029/2006GL028040.

Krismer, T. R., M. A. Giorgetta, and M. Esch (2013), Seasonal aspects of the quasi-biennial oscillation in the Max Planck Earth System Model and ERA-40, *J. Adv. Model. Earth Syst.*, *5*, doi:10.1002/jame.20024.

Marshall, A., and A. A. Scaife (2009), Impact of the quasi-biennial oscillation on seasonal forecasts, *J. Geophys. Res.*, *114*, D18110, doi:10.1029/2009JD011737.

Molteni, F., T. Stockdale, M. Balmaseda, G. Balsamo, R. Buizza, L. Ferranti, L. Magnusson, K. Mogensen, T. Palmer and F. Vitart (2011), The new ECMWF seasonal forecast system (System 4). ECMWF Technical Memorandum 656. [Available from http://www.ecmwf.int/publications.]

Pascoe, C. L., L. J. Gray, and A. A. Scaife (2005), A GCM study of the influence of equatorial winds on the timing of sudden stratospheric warmings, *Geophys. Res. Lett.*, *33*, L06825, doi:10.1029/2005GL024715.

Pohlmann, H., W. A. Müller, K. Kulkarni, M. Kameswarrao, D. Matei, F. Vamborg, C. Kadow, S. Illing, and J. Marotzke (2013), Improved forecast skill in the tropics in the new MiKlip decadal climate predictions, *Geophys. Res. Lett.*, *40*, 5798–5802, doi:10.1002/2013GL058051.

Reed, R. J., W. J. Campbell, L. A. Rasmussen, and D. G. Rogers (1961), Evidence of downward-propagating annual wind reversal in the equatorial stratosphere, *J. Geophys. Res.*, *66*, 813–818.

Scaife, A. A., N. Butchart, C. D. Warner, D. Stainforth, W. A. Norton, and J. Austin (2000), Realistic quasi-biennial oscillations in a simulation of the global climate, *Geophys. Res. Lett.*, *27*, 3481–3484.

Scaife A. A., N.Butchart, C. D. Warner and R. Swinbank (2002), Impact of a spectral gravity wave parameterization on the stratosphere in the Met Office Unified Model. *J. Atm. Sci.*, *59*, 1473–1489.

Scaife, A. A., D. Copsey, C. Gordon, C. Harris, T. Hinton, S. J. Keeley, A. O'Neill, M. Roberts, and K. Williams (2011), Improved atmospheric blocking in a climate model, *Geophys. Res. Lett.*, *38*, L23703, doi:10.1029/2011GL049573.

Scinocca, J. F., N. A. McFarlane, M. Lazare, J. Li, and D. Plummer (2008), Technical Note: The CCCma third generation AGCM and its extension into the middle atmosphere, *Atmos. Chem. Phys.*, *8*, 7055–7074, doi:10.5194/acp-8-7055-2008.

Scott, R. K., and P. H. Haynes (1998), Internal interannual variability of the extratropical stratospheric circulation: The low-latitude flywheel, *Q. J. R. Meteorol. Soc.*, *124*, 2149–2173.

Smith, D. M., S. Cusack, A. W. Colman, C. K. Folland, G. R. Harris, and J. M. Murphy (2007), Improved surface temperature prediction for the coming decade from a global climate model, *Science*, *317*, 796–799, doi:10.1126/science.1139540.

Smith, D. M., R. Eade, N. J. Dunstone, D. Fereday, J. M. Murphy, H. Pohlmann, and A. A. Scaife (2010), Skilful multi-year predictions of Atlantic hurricane frequency, *Nat. Geosci.*, *3*, 846–849, doi:10.1038/NGEO1004.

Smith, D., A. A. Scaife, and B. Kirtman (2012), What is the current state of scientific knowledge with regard to seasonal and decadal forecasting?, *Env. Res. Lett.*, *7*, 015602, doi:10.1088/1748-9326/7/1/015602.

Stevens, B., et al. (2013), Atmospheric component of the MPI-M Earth System Model: ECHAM6, *J. Adv. Model. Earth Syst.*, *5*, 146–172, doi:10.1002/jame.20015.

Thompson, D. W. J., M. P. Baldwin, and J. M. Wallace (2002), Stratospheric connection to Northern Hemisphere wintertime weather: Implications for prediction, *J. Clim.*, *15*, 1421–1428.

Uppala, S. M., et al. (2005), The ERA-40 re-analysis, *Quart. J. R. Meteorol. Soc.*, *131*, 2961–3012, doi:10.1256/qj.04.176.

Veryard, R. G., and R. A. Ebdon (1961), Fluctuations in tropical stratospheric winds, *Meteorol. Mag.*, *90*, 125–143.

Walters, D. N., et al. (2011), The Met Office Unified Model Global Atmosphere 3.0 and JULES Global Land 3.0/3.1 configurations, *Geosci. Model Dev. Discuss.*, *4*, 1213–1271.

Warner, C. D., A. A. Scaife, N. Butchart, and R. Swinbank (2005), Filtering of parameterized nonorographic gravity waves in the Met Office Unified Model, *J. Atm. Sci.*, *62*, 1831–1848.

Wilson, D. R., A. C. Bushell, A. M. Kerr-Munslow, J. D. Price, and C. J. Morcrette (2008), PC2: A prognostic cloud fraction and condensation scheme. I: Scheme description, *Q. J. R. Meteorol. Soc.*, *134*, 2093–2107, doi:10.1002/qj.333.

Yamashita, Y., H. Akiyoshi, and M. Takahashi (2011), Dynamical response in the Northern Hemisphere midlatitude and high-latitude winter to the QBO simulated by CCSR/NIES CCM, *J. Geophys. Res.*, *116*, D06118, doi:10.1029/2010JD015016.